

# Curved FtsZ protofilaments generate bending forces on liposome membranes

Masaki Osawa\*, David E Anderson  
and Harold P Erickson\*

Department of Cell Biology, Duke University Medical Center, Durham, NC, USA

**We have created FtsZ-YFP-mts where an amphipathic helix on the C-terminus tethers FtsZ to the membrane. When incorporated inside multi-lamellar tubular liposomes, FtsZ-YFP-mts can assemble Z rings that generate a constriction force. When added to the outside of liposomes, FtsZ-YFP-mts bound and produced concave depressions, bending the membrane in the same direction as the Z ring inside liposomes. Prominent membrane tubules were then extruded at the intersections of concave depressions. We tested the effect of moving the membrane-targeting sequence (mts) from the C-terminus to the N-terminus, which is approximately 180 degrees from the C-terminal tether. When mts-FtsZ-YFP was applied to the outside of liposomes, it generated convex bulges, bending the membrane in the direction opposite to the concave depressions. We conclude that FtsZ protofilaments have a fixed direction of curvature, and the direction of membrane bending depends on which side of the bent protofilament the mts is attached to. This supports models in which the FtsZ constriction force is generated by protofilament bending.**

*The EMBO Journal* (2009) 28, 3476–3484. doi:10.1038/emboj.2009.277; Published online 24 September 2009

**Subject Categories:** membranes & transport; structural biology  
**Keywords:** bar domain; cytoskeleton; dynamin; FtsZ; liposome

## Introduction

The tubulin homologue FtsZ is the major cytoskeletal protein in bacterial cytokinesis. At the level of light microscopy, FtsZ assembles into a thin ring under the inner bacterial membrane. This Z ring provides the cytoskeletal framework for docking the other proteins of the division machine, many of them involved in remodelling the peptidoglycan wall. That FtsZ provided the cytoskeletal framework for the cytokinetic machine was first suggested by its localization to the forming septum (Bi and Lutkenhaus, 1991), the discovery that it was a homologue of tubulin (de Boer *et al*, 1992; RayChaudhuri and Park, 1992; Mukherjee *et al*, 1993), and that it could assemble into filaments *in vitro* (Mukherjee and Lutkenhaus, 1994). Ten years ago Erickson *et al* (1996; 1997) suggested the Z-centric hypothesis that FtsZ may also

generate the constriction force that leads to septation. This hypothesis was confirmed by our recent demonstration that FtsZ incorporated into tubular liposomes can assemble Z rings that generate a constriction force, in the absence of any other proteins (Osawa *et al*, 2008).

That study made use of the discovery by Pichoff and Lutkenhaus (2005) of the mechanism by which FtsZ is normally tethered to the membrane. FtsZ has a short peptide on its C-terminus that binds FtsA, and FtsA has a short amphipathic helix on its C-terminus that inserts into the lipid bilayer. Thus, FtsA tethers FtsZ to the membrane. We made a membrane-targeted FtsZ by removing its FtsA-binding peptide and replacing it with an amphipathic helix. This membrane-targeted FtsZ could tether itself to the membrane. It was able to assemble Z rings when expressed in *Escherichia coli*, and assembled contractile Z rings when incorporated inside tubular liposomes *in vitro*.

As we were developing that study, we discovered that membrane-targeted FtsZ could also generate a bending force and distort membranes by binding to the outside of liposomes. The FtsZ-mts formed concave invaginations on the liposome and then extruded it into multiple thin tubules. To explore the mechanism of the membrane force, we moved the membrane-targeting sequence (mts) from the C-terminus to the N-terminus, and discovered that it then formed convex bulges on the liposomes. Here we describe these membrane deformation phenomena and suggest that the force generation on the inside and outside of liposomes involves a common mechanism of bending by FtsZ protofilaments.

## Results

### **Membrane-targeted FtsZ tubulates liposomes *in vitro***

We purified the FtsZ-YFP-mts protein and mixed it with liposomes produced from *E. coli* lipids. FtsZ-YFP-mts could bind to the outside of liposomes without GTP (Figure 1A). When GTP was added, the liposomes were deformed and sprouted long filamentous structures or tubules (Figure 1B). This phenomenon is totally different from the formation of Z rings inside ‘large tubular liposomes,’ which we previously reported (Osawa *et al*, 2008). Those large tubular liposomes appeared to be produced by shearing forces when the coverslip was applied, and they occasionally trapped FtsZ on the inside and assembled Z rings. The tubules studied here are produced by FtsZ on the outside, and are ~50–200 nm in diameter, compared with the ~2000-nm diameter of the large, multi-lamellar, tubular liposomes. Tubulation was only observed when the concentration of FtsZ-YFP-mts was above 1  $\mu\text{M}$ , which is somewhat above the 0.7- $\mu\text{M}$  critical concentration for assembly of FtsZ in solution (Chen and Erickson, 2005). Time-lapse imaging showed that the tubules elongated at a rate of ~0.5  $\mu\text{m}/\text{min}$ , equivalent to protofilaments elongating at two FtsZ subunits per second (Figure 1C). The tubules maintained constant brightness along their length as they grew longer. This suggests that the surfaces

\*Corresponding authors. M Osawa or HP Erickson, Department of Cell Biology, Duke University Medical Center, Durham, NC 27710-3709, USA. Tel.: +1 919 684 6385; Fax: +1 919 684 8090; E-mails: m.osawa@cellbio.duke.edu or h.erickson@cellbio.duke.edu

Received: 13 February 2009; accepted: 18 August 2009; published online: 24 September 2009

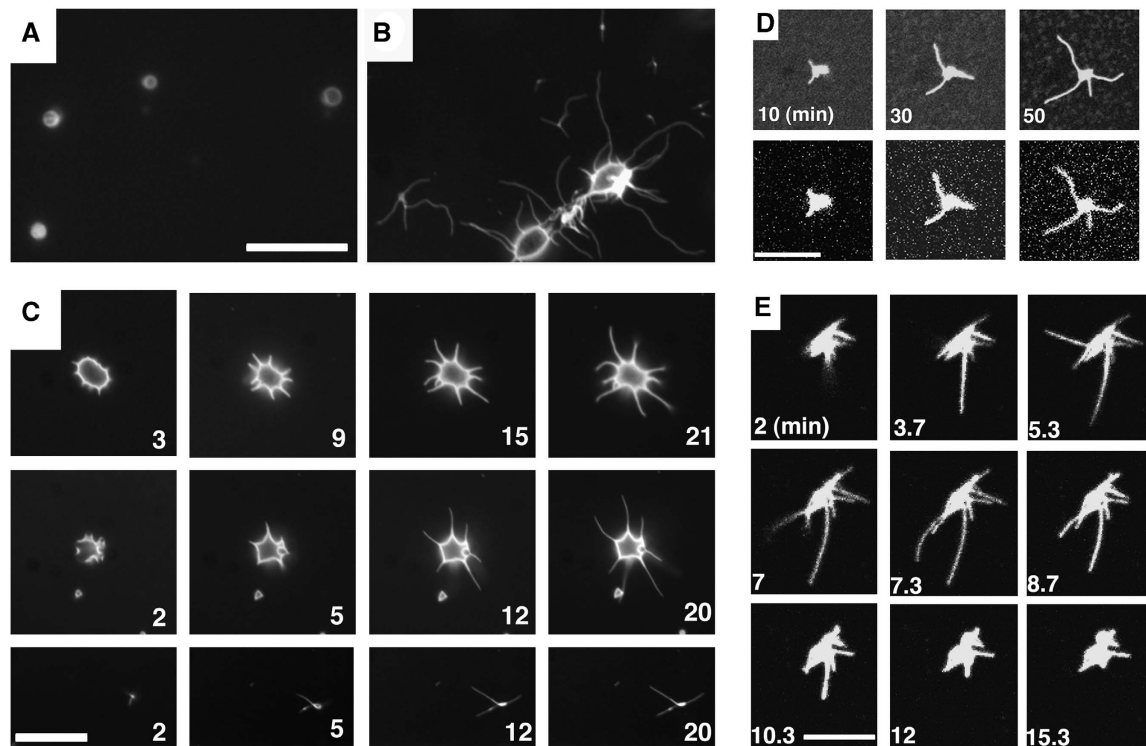


**Figure 1** Membrane tubulation of liposomes by FtsZ-mts and FtsZ-YFP-mts. (A) Liposomes prepared from *E. coli* Polar Lipid Extract were mixed with 4  $\mu$ M FtsZ-YFP-mts in HMK100 buffer without GTP. (B) GTP at 400  $\mu$ M was then added to the mixture and images were obtained after 40 min. (C) Liposomes prepared from mixtures of PC with 20% DOPG in HMK100 were treated with 4  $\mu$ M FtsZ-YFP-mts and 400  $\mu$ M GTP. Time-lapse images were recorded starting at 2 or 3 min. Large, multi-lamellar liposomes are shown in the upper and middle panel, and a small liposome is shown in the lower panel. (D) Liposomes prepared from 100% PC were stained with DiD. Tubulation was generated with 4  $\mu$ M FtsZ-YFP-mts, 400  $\mu$ M GTP in HMK350. Tubulating liposomes were imaged both for YFP (upper panel) and DiD (lower panel). Lipid and YFP are co-localized on the liposome and tubules. (E) Vesicle tubulation was also generated by FtsZ-mts (without the YFP tag—these were imaged with DiD). With 20  $\mu$ M FtsZ-mts and 400  $\mu$ M GTP the tubules formed and elongated for about 7 min, then retracted. Scale bars are 10  $\mu$ m.

of the liposome and tubules are saturated with FtsZ filaments, and the total brightness of the liposome plus tubules grows as the total surface area increases during growth of the tubules.

To confirm that FtsZ is on the outside of the tubulating liposomes, we used the small polar fluorescent dye HccA (7-hydroxycoumarin-3-carboxylic acid; Invitrogen) to test the leakiness of the liposomes. We mixed HccA with liposomes and then added FtsZ-YFP-mts and GTP. Many tubulating liposomes were found that contained no HccA, as indicated by a dark profile on the background of fluorescence (data not shown). Conversely, when we washed away the exterior fluid from the liposomes, all fluorescence disappeared from the liposomes (data not shown). The multi-lamellar tubular liposomes that showed reconstitution of Z rings in our previous study were prepared in higher salt, and were much more leaky to HccA and proteins than the thinner-walled liposomes used in the present study (Osawa and Erickson, 2009).

To explore how the binding and tubulation are affected by the nature of the lipids, we prepared liposomes from 1,2-dioleoyl-*sn*-glycero-3-{phospho-*rac*-(1-glycerol)} (DOPG, negatively charged) and/or phosphatidylcholine (PC, zwitterionic and neutral). Liposomes prepared from 100% PC did not bind FtsZ-YFP-mts without GTP. This is consistent with the previous observation that the monomeric mts from *E. coli* MinD did not bind to zwitterionic lipids PC and phosphatidylethanolamine (Szeto *et al*, 2003). However, when GTP was added, the FtsZ-YFP-mts could bind and

tubulate the pure PC liposomes. Liposomes prepared from a 20:80 mixture of DOPG:PC responded identically to liposomes prepared from *E. coli* lipid in these assays (Figure 1C), that is, they could bind FtsZ-YFP-mts in the absence of GTP and tubulate when GTP was added. All lipid vesicles showed tubulation only above 1  $\mu$ M FtsZ-YFP-mts.

To confirm that the sprouting tubules contain both FtsZ and lipid, we labelled the 100% PC liposomes with the red fluorescent dye DiD (1,1'-dioctadecyl-3,3,3',3'-tetramethylindodicarbocyanine perchlorate; Invitrogen) and separately imaged the YFP and DiD. Figure 1D shows that protein and lipid are colocalized on both the liposome and the tubules. Finally, we tested whether FtsZ-mts, without the YFP, could tubulate liposomes. Figure 1E shows that it can. In this experiment we used 20  $\mu$ M FtsZ-mts, which we estimated would consume the 400  $\mu$ M GTP in several minutes. The tubules grew for about 7 min and then retracted, presumably as the GTP was used up (Figure 1E).

We measured the GTPase activity of all constructs. GTPase activities were only detected above 0.5  $\mu$ M, which is similar to the critical concentration of GTPase activity for wild-type FtsZ (Redick *et al*, 2005). The GTPase activities (at 30°C) were as follows (expressed as GTP per FtsZ per min): wild-type FtsZ, 5.5; FtsZ-mts, 2.6; FtsZ-YFP-mts (native preparation), 3.6 and FtsZ-YFP-mts (renatured preparation), 1.3. The FtsZ constructs with mts tended to form protofilament bundles (data not shown), which we have found reduces the GTPase (Chen and Erickson, 2009).

When FtsZ-YFP-mts was maintained at a constant  $4\ \mu\text{M}$  and the liposome concentration was increased, the tubulation disappeared above a certain amount of lipid. For this experiment, we used small liposomes prepared with the extruder, which could be reliably quantitated. The maximum molar ratio of lipid to FtsZ-YFP-mts that could support tubulation was 100:1 for DOPG and 30:1 for PC.

### Membrane-targeted FtsZ forms concave depressions on the surface of liposomes

We noticed that the liposomes frequently showed concave depressions between the sprouting tubules, and prior to growth of tubules (Figure 1C, middle panel). Figure 2A shows a particularly clear example of multiple concave depressions formed on large, elongated liposomes. Figure 2B shows a long, tubular liposome similar to those that assembled Z rings when FtsZ-YFP-mts was inside (Osawa *et al*, 2008). The liposomes in Figure 2B seem to have FtsZ-YFP-mts only on the outside. FtsZ-YFP-mts is clustered in patches, most of which are forming concave depressions (arrows). This liposome had higher contrast in DIC (not shown) than those in Figure 2A, which suggests a thicker wall. The concavities are much shallower than those in Figure 2A, perhaps reflecting the stiffness of the thicker wall. Figure 2C shows similar concave depressions on a large spherical multi-lamellar liposome.

To enhance the formation of concave depressions, we made liposomes in a lower-salt buffer, which favours formation of unilamellar or thinner-walled liposomes. Concave depressions were better seen at lower FtsZ concentrations; at higher FtsZ tubulation was the dominant reaction. Figure 2D and E shows a large, spherical liposome that has many concave FtsZ patches. Figure 2D is focused on the middle of the liposome, and Figure 2E on the upper surface, which shows the patches most clearly. Figure 2F and G show two examples in which the concave patches appear to have invaginated into the interior of the large mother liposome. Some of these appear to be still connected to the surface, whereas some may have pinched off. Occasionally we found large liposomes that had invaginated many small spherical liposomes (Figure 2H). This may happen when the coverslip is applied, since we have not found examples that we could follow over time. The small internal liposomes appear to be connected to each other in linear arrays, probably by a membrane extension, which eventually connects to the surface of the large liposome (Figure 2I).

Although FtsZ-YFP-mts was able to bind to liposomes at a similar level with or without GTP, judging from the fluorescence brightness, the patchy structures and concavities appeared only when GTP was added. This indicates that FtsZ assembly is required to form concave depressions. The concave depressions were observed on the surface of both spherical unilamellar liposomes produced by a low-salt buffer, and on thin multi-lamellar liposomes (data not shown). When vesicles were made at one salt concentration and incubated with FtsZ at another salt concentration, concave depressions were observed under both hyper- and hypo-osmotic conditions ( $\pm 40\ \text{mOsM}$ , data not shown), indicating that this phenomenon is independent of osmotic pressure within this range.

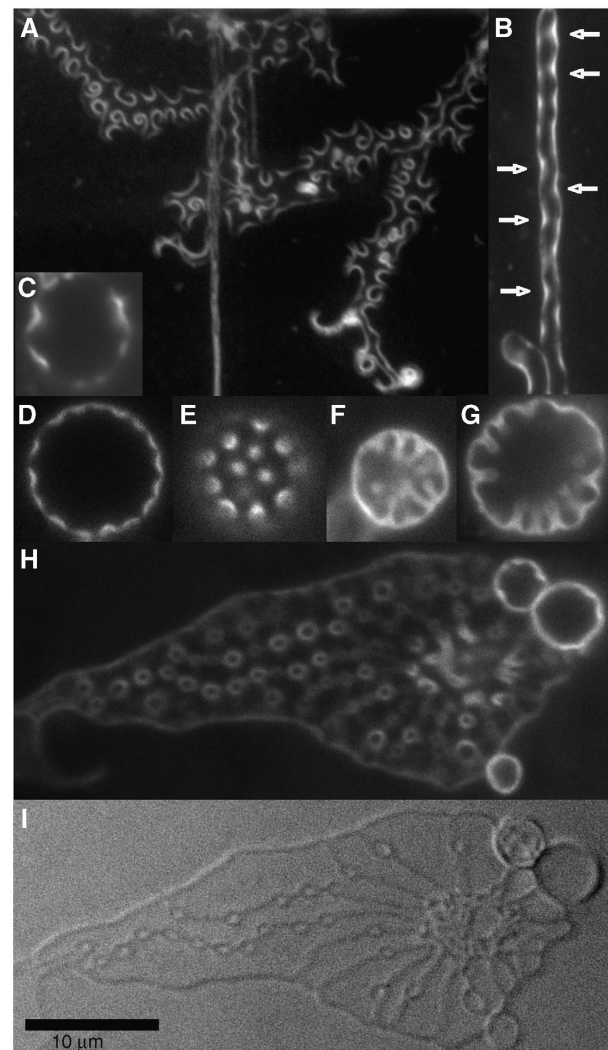


**Figure 2** Concave depressions formed on liposomes by FtsZ-YFP-mts. Liposomes produced from 80% egg PC with 20% DOPG were mixed with  $4\ \mu\text{M}$  FtsZ-YFP-mts and  $400\ \mu\text{M}$  GTP in reaction buffer HMKCG. (A) Large elongated liposomes showing multiple deep concavities over their surfaces. (B) A thicker-walled tubular liposome with FtsZ on the outside. This is similar to the liposomes that formed Z rings on the inside, but here the FtsZ seems to be bound on the outside forming concave patches. The concavities are shallower on this thicker-walled liposome. (C) A large spherical multi-lamellar liposome showing concave depressions. (D, E) A large, thin-walled liposome prepared and reacted in a low-salt reaction buffer (HMK100, with 10% glycerol). The focus is on a plane through the middle of the liposome (D) or on its upper surface (E), the latter showing the concave patches in face view. (F, G) In some liposomes the concavities invaginated deeply into the interior, and some may have pinched off. (H) Occasional large liposomes contained many small spherical liposomes apparently produced by invagination and pinching off. (I) A differential interference contrast image showing that the small liposomes are connected to each other in linear arrays, which eventually reach the surface of the large enclosing liposome.

### Arrangements of FtsZ filaments on concave and tubulated liposomes

Negative-stain EM showed tubular extensions projecting from liposomes (Figure 3A and B). The tubules were typically  $\sim 200\ \text{nm}$  wide, consistent with the very thin appearance under light microscopy. Most liposomes and tubular extensions showed no substructure that could be related to FtsZ,

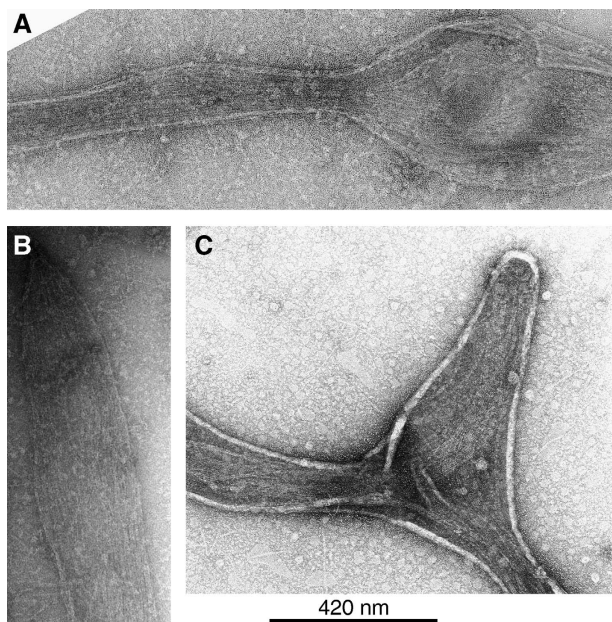


**Figure 3** EM images of negative stained tubulating liposomes. (A, B) Liposomes produced from 80% egg PC with 20% DOPG were tubulated with 4  $\mu$ M FtsZ-YFP-mts and 400  $\mu$ M GTP for 7 min in reaction buffer HMK100. Parallel filaments were formed on the membrane tubules. (C) *E. coli* lipid vesicles were tubulated with 3  $\mu$ M FtsZ-mts and 400  $\mu$ M GTP for 1 min in reaction buffer HMK100. Curved filaments and sheets of filaments are visible over the concavities and tubular extensions. Some sheets are overlapping and one at the bottom is clearly curved.

but in some areas we found what looked like sheets of protofilaments, which were generally aligned parallel to the long axis of the tubules. Figure 3C shows a liposome 1 min after addition of GTP. It has concave indentations similar to those observed by light microscopy, and tubules are beginning to project from the intersection of the concavities. There are sheets of protofilaments lying along the indentations and the initiating tubules. Typical FtsZ protofilaments, one-subunit thick, were seen on the carbon film between vesicles with both FtsZ-mts and FtsZ-YFP-mts.

#### Subunit turnover of FtsZ on the tubulating membranes

FtsZ filaments *in vitro* and the Z ring *in vivo* are highly dynamic, with a half-time for subunit exchange of 6–9 s (Anderson *et al*, 2004; Chen and Erickson, 2005). We measured the exchange rates of FtsZ-YFP-mts on the tubulating liposomes using a fluorescence recovery after photobleaching (FRAP) assay (Figure 4A). Liposomes made from 100% PC were chosen for these experiments, because we found that FtsZ-YFP-mts could not bind to these liposomes without GTP. The extended tubules and the central spherical regions of the liposomes had similar recovery times after bleaching. Recovery could be fit to single-exponential curves with a half-time of  $25.4 \pm 5.0$  s ( $n = 6$ ) on tubulating regions (Figure 4C). This is about four times slower than the turnover times for *E. coli* FtsZ protofilaments in solution (Chen and Erickson, 2005). This slower turnover may be due to the direct attachment of each FtsZ-YFP-mts subunit to the membrane. We also noted that the boundary of the bleached and unbleached areas remained sharp during the recovery, and recovery appeared uniform throughout the bleached

region, suggesting that the recovery involved exchange with FtsZ in the solution, and not diffusion of FtsZ along the lipid.

#### Tubulation of liposomes by FtsZ with minimal GTPase activity

We previously reported that FtsZ hydrolyses GMPCPP 3–10 times slower than GTP (Romberg *et al*, 2001). We have recently repeated this measurement and found that the hydrolysis rate in 100 mM KAc, pH 7.7, was actually 50 times slower (0.08 per min per FtsZ for GMPCPP, versus 4 per min for GTP, C Sontag and H Erickson, unpublished results). Here we found that GMPCPP could support tubulation of lipid vesicles with a growth rate ( $\sim 0.5 \mu\text{m}/\text{min}$ ) identical to that of GTP (Figure 4B). This suggests that GTP hydrolysis is not rate-limiting and perhaps not necessary for tubulation.

We used FRAP to measure exchange on tubules formed with GMPCPP. In GMPCPP, only 10% of the YFP signal recovered over 10 min (Figure 4B and D), suggesting that GTP hydrolysis is essential for rapid exchange of FtsZ-YFP-mts. Figure 4E shows an experiment in which the entire GMPCPP-tubulating liposome was bleached. At 300 s there was minimal recovery on the liposome and tubules, but bright fluorescence appeared over time at the tips of tubules. This reflects elongation of the tubules. The new FtsZ is inserted at the tip, rather than at the junction of the tubule with the vesicle or along the length of the tubule (Figure 4E).

#### Moving the mts from the C-terminus to the N-terminus reverses the direction of membrane curvature

In FtsZ-YFP-mts the C-terminal (YFP-) mts follows amino acid (aa) A366. The 50-aa segment M317-A366 is unstructured in crystal structures and is thought to be a flexible tether between the FtsA-binding peptide (replaced here with mts) and the globular domain. This tether is attached to G316, the last aa visible in crystal structures (Cordell *et al*, 2003). If protofilament bending is the source of the bending force on the membrane, moving the tether-mts to another site on the globular domain might alter the membrane binding. To test this we engineered the simplest change, moving the mts from the C-terminus to the N-terminus. The first nine aa's of the N-terminus are also invisible in crystal structures (Cordell *et al*, 2003) and presumed unstructured. We made two constructs with an N-terminal mts. The first had one aa between the mts and the N-terminal methionine of FtsZ, making a short tether 10-aa long (including the nine aa's from FtsZ). The second inserted 43 aa's, making a tether 52-aa long. Figure 5 shows that each of these N-terminal mts constructs bound to the outside of liposomes and produced convex protrusions, the opposite of the concave depressions produced by the C-terminal mts. The length of tether did not affect the production of the convex bulges. These convex protrusions were also observed on unilamellar liposomes and under both hyper- and hypo-osmotic conditions (data not shown).

## Discussion

#### *In vitro* tubulation of liposomes

The reconstitution of contractile Z rings inside tubular liposomes was an important step towards reconstruction of the cell division machinery *in vitro* (Osawa *et al*, 2008). As we

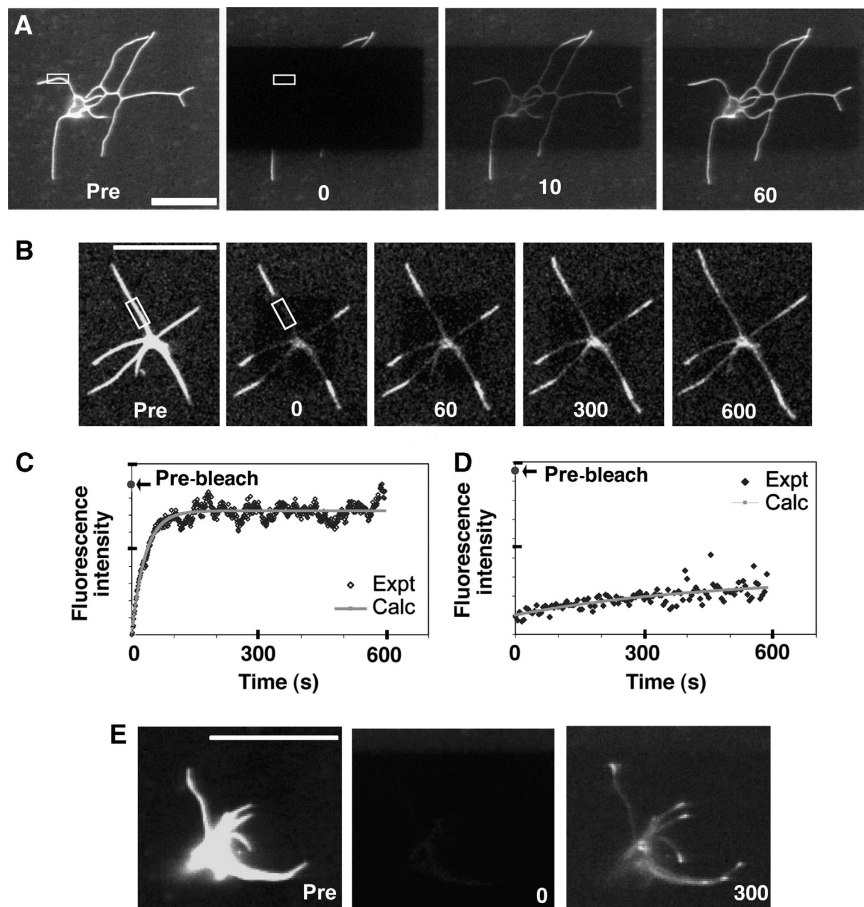


**Figure 4** FRAP assays of tubulating liposomes. (A) 100% PC liposomes were tubulated with 4  $\mu$ M FtsZ-YFP-mts and 400  $\mu$ M GTP in HMK350. The liposome and most of the projecting tubules were bleached at time 0 and recovery was imaged over 600 s. (B) GMPCPP at 400  $\mu$ M was used instead of GTP. (C, D) The fluorescence recoveries within the rectangles in panels A and B are shown for GTP (C) and GMPCPP (D). (E) A tubulating liposome with GMPCPP was entirely bleached. Bright fluorescence appeared at the tips of the tubules, indicating continued growth by addition of FtsZ at the tip. Scale bars are 10  $\mu$ m.

were investigating the interaction of FtsZ with liposomes, we discovered that FtsZ-YFP-mts could produce concave depressions and tubulate liposomes when added to the outside.

A variety of proteins can tubulate lipid vesicles. Dynamin forms small ( $\sim$ 50 nm diameter) membrane tubules by assembling a distinctive helical array that wraps around the outside of the membrane tubules (Sweitzer and Hinshaw, 1998). Proteins containing a BAR domain can also tubulate liposomes, and like dynamin they form helical filaments that wrap around the outside of the tubules. The BAR domains are banana-shaped helical bundles that curve the membrane by binding with their concave surface to the outer surface of the membrane (Takei *et al*, 1998; Farsad and De Camilli, 2003; Shimada *et al*, 2007). A subclass of BAR domains, called I-BAR, also tubulates liposomes, but bends the membrane in the opposite direction. Thus, the I-BAR domains bind the membrane on their convex surface and form an array on the inside of the tubules (Saarikangas *et al*, 2009). BAR domains bind the membrane by a group of positively charged aa's on the concave surface; for I-BAR domains the positive aa's are on the convex surface.

The most relevant tubulation system for our consideration is MinD itself, since we used the amphipathic helix from MinD as the membrane tether for FtsZ. Hu *et al* (2002) found that MinD plus ATP tubulated liposomes by forming

polymers that wrapped circumferentially around the tubules. In contrast to dynamin, BAR domains and MinD, where the polymers wrap circumferentially around the membrane tubules, the FtsZ-mts protofilaments seem aligned parallel to the axis of the tubules. Recently Dajkovic *et al* (2008) demonstrated a similar axial arrangement of filaments when liposomes were tubulated by an equimolar (6  $\mu$ M) mixture of FtsZ, MinD and MinC. In this mixed system, the lipid concentration was increased to a point where 6  $\mu$ M MinD alone would not tubulate (Dajkovic *et al*, 2008). We suggest that the tubulation in this mixed system is driven by FtsZ assembly, with the MinC-MinD providing just the tether to the membrane. This would account for the filaments running parallel to the tubule axis, the same as in our system with directly tethered FtsZ-mts.

#### **Direction of the force on the membrane**

Z rings on the inside of tubular liposomes are bound to the concave membrane surface and constrict it to a more concave curvature (smaller diameter). How is this related to the forces on membranes generated by FtsZ-mts on the outside? A key observation is that the initial distortion of the membrane is the formation of concave depressions. These concave depressions on the outside would require a bending force on the membrane in the same direction as the Z ring on the inside

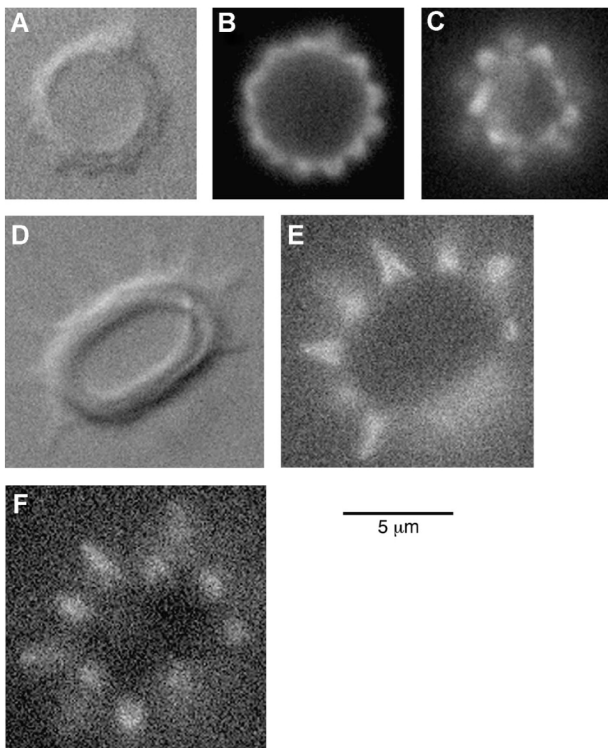
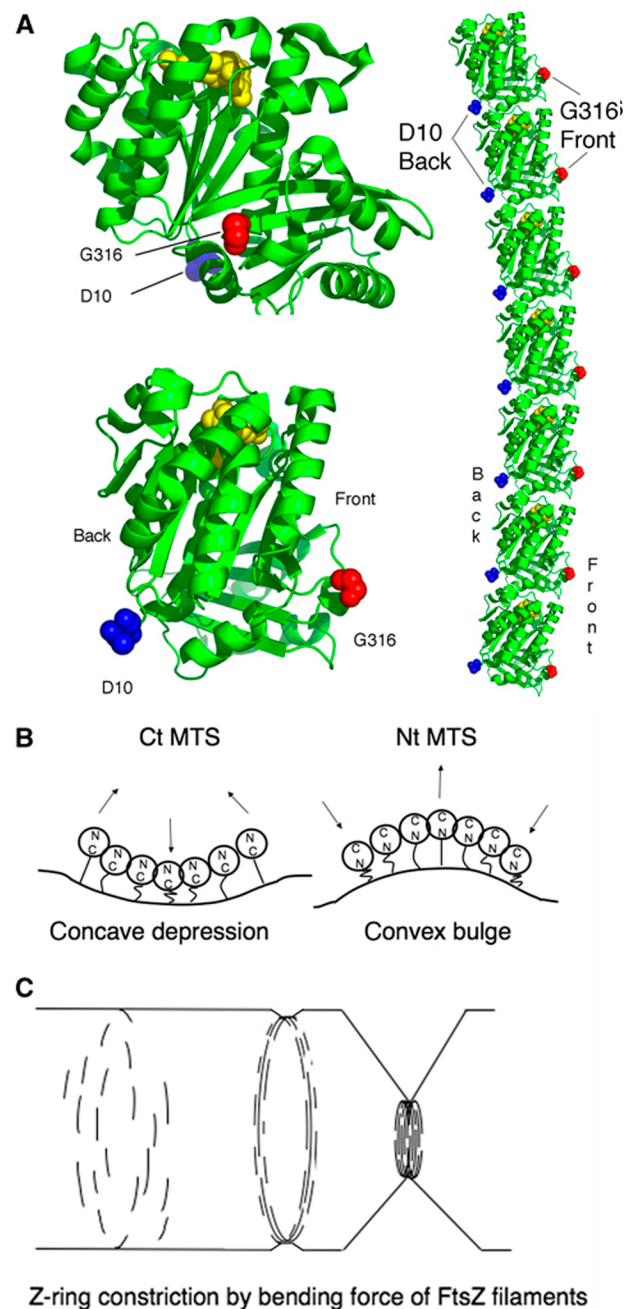


**Figure 5** Convex protrusions formed on liposomes by mts-FtsZ-YFP where the mts and tether is switched from the C-terminus to the N-terminus. The focus is on a plane through the middle of the liposome (B, E) or on its upper surface (C, F), the latter showing the convex patches in face view. The mts-FtsZ-YFP with a 45-aa linker was used in panels A–C and a 2-aa linker was used in D–F. Liposomes produced from 80% egg PC with 20% DOPG were mixed with 10 μM (for the mts with a 45-aa linker) or 15 μM (for the mts for a 2-aa linker) mts-FtsZ-YFP and 1 mM GTP in a low-salt reaction buffer (HMK100 with 10% glycerol), which is essentially the same as in Figure 2D and E.

**Figure 6** (A) A molecular model of FtsZ showing the attachment points of tethers at the C- and N-terminal positions. The model is from *Pseudomonas* FtsZ (pdb: 10 fu; Cordell *et al*, 2003) visualized with PyMol (DeLano, WL The PyMOL Molecular Graphics System (2002) on World Wide Web, <http://www.pymol.org>). The top left model shows the FtsZ from the ‘front’ view, as tubulin appears from the outside of a microtubule. The lower left shows the FtsZ from the left side. The normal C-terminal tether emerges from aa G316 on the front surface. The artificial N-terminal tether that we created is attached to the N-terminal methionine, continues through a short linker and is anchored to D10, the first aa visible in the crystal structure. These two attachment points are on the front and back faces, approximately 180 degrees apart. The right-hand model shows FtsZ subunits connected into a curved protofilament, with a 5-degree bend (5 degrees was arbitrarily chosen to illustrate the direction of curvature) at each interface, viewed from the left. The C-terminal attachment G316 is on the convex surface labelled ‘front’ and the N-terminal attachment is on the concave surface. A coloured version of this figure is available at *The EMBO Journal* online. (B) A model of membrane deformations generated by bending force of FtsZ filaments. When the mts is attached at the C- or N-terminus, the bent protofilaments form a concave depression (left panel) or convex bulge (right panel), respectively. The direction of bending to make a concave depression is the same as that of Z-ring constriction. (C) A model of Z-ring constriction by FtsZ filaments that have a preferred curvature. The scheme to the left shows FtsZ filaments scattered on the cylindrical membrane; because of their curvature they will align circumferentially. The scheme in the middle shows the filaments approaching each other and coalescing to make a Z ring. The scheme to the right shows the ring constricting.

(Figure 6B and C). A simple mechanism for bending the membrane would be for the FtsZ protofilaments themselves to have a preferred bent conformation, which generates a bending force on the attached membrane (Erickson *et al*, 1996; Erickson, 1997; Allard and Cytrynbaum, 2009). Our observations now favour a bending mechanism over alternative models based on lateral bonds and sliding protofilaments (discussed in Erickson, 2009).

The idea that the concave depressions are generated by a preferred curvature of the bound protofilaments, is supported by our discovery that switching the mts from the C to the N-terminus switched the membrane distortion from concave depressions to convex protrusions. The geometry of mts attachment is shown in Figure 6A. The tether attaching the C-terminal mts to the globular FtsZ domain is anchored to



the front of the globular FtsZ domain, corresponding to the outside of a microtubule. When the tether is switched to the N-terminus it is anchored to the back, approximately 180 degrees away. To explain the concave and convex bending of the membrane, we propose that the FtsZ protofilament has a preferential bend, with the C-terminal tether attachment on the convex side (Figure 6A). If the mts extends from the convex side of the protofilament, it will generate a concave depression in the membrane, and if it extends from the concave side of the protofilament it will generate a convex protrusion (Figure 6B). An implicit assumption is that the tether-*mts* binds the membrane on the face to which it is anchored, rather than looping around the protofilament.

There is now evidence for at least two curved conformations of FtsZ protofilaments, discussed in more detail by Erickson (2009). A highly curved conformation with a 22-degree bend between subunits produces mini-rings on cationic lipid monolayers and helical tubes in DEAE dextran, both measuring ~24 nm in outside diameter. An intermediate curved conformation with a 2.5-degree bend produces a circular form of ~200 nm in diameter. The concave depressions and convex protrusions of the membranes are on the order of 1000 nm in diameter. This is similar to the diameter of an undivided bacterium, and much less curved than either curved protofilament conformation. We therefore suggest that, in the liposome system, the protofilaments are only able to bend the membranes a fraction of the way towards their preferred curvature. (We also note that the relation of these curved conformations to GTP hydrolysis is more complex than the earlier proposal, and is not yet understood; Erickson, 2009.)

One problem raised by the curved protofilament model in Figure 6 is that its direction of curvature is opposite of what we expect by analogy to tubulin rings. Tubulin rings are curved perpendicular to the wall of the microtubule, leaving the outside, kinesin-binding face of the microtubule on the inside of the ring (Wang and Nogales, 2005; Moores and Milligan, 2008; Tan *et al*, 2008). In order for FtsZ-*mts* to make concave depressions on the membrane, we had to put the corresponding face on the outside of the ring (Figure 6A). One possibility is that the membrane bending is not produced by the highly curved, mini-ring conformation, but by the intermediate curved conformation. We have no information about the direction of this curvature, and it could be in the opposite direction to the highly curved.

Another consideration is the structure of the supposedly flexible tether linking the globular domains to the membrane. A tether of 50 aa's would be 17 nm long if fully extended. It would seem that a flexible tether this long would easily permit the protofilament to roll over on its side and bend in the plane of the membrane, without generating any bending force on the membrane. However, a chain of unstructured aa's behaves as a worm-like chain and tends to collapse on itself. The average end-to-end length of a 50-aa peptide is ~4 nm (Ohashi *et al*, 2007). The worm-like chain will behave as an entropic spring that will generate a force if its ends are extended. Bustamante *et al* (1994) provide a formula that calculates a force of 10 pN to be needed to stretch the end-to-end distance to one-half of its contour length (a persistence length 0.5 nm was used for this calculation). Lan *et al* (2007) estimated that a force of ~8 pN would be

needed to divide cells. The force of this entropic spring is similar in magnitude and may be sufficient to keep the front face of the protofilament facing the membrane.

The concave depressions and the convex bulges are incomplete arcs of membrane, which provides another argument that the force is generated by bending protofilaments. Mechanisms where contraction is produced by sliding of protofilaments (Horger *et al*, 2008; Lan *et al*, 2009) would not be able to generate concavities, since the filaments are only tethered to the fluid bilayer and would be free to slide without generating force.

The concave depressions are the first membrane distortions formed, and in most conditions they are followed by tubules extruding from the vertices of the concavities. The extrusion of tubules is probably related to the bending that forms concave depressions, but the mechanism is not yet clear. Our preliminary assumption is that the vertices of the concavities are surrounded by FtsZ protofilaments or sheets aligned parallel to the axis of the initial tubule, all trying to bend the membrane outward. However, because they are balanced on all sides, the net result may be to pull membrane from the liposome into the growing tubule. We should note also that FtsZ with the *mts* on the N-terminus also produced tubules, but much fewer than with the C-terminal *mts* (data not shown). It is not clear how tubulation could be generated by bending forces in these opposite directions.

We now have two *in vitro* reconstitution systems for investigating how FtsZ interacts with the membrane and generates force on it. The Z rings inside tubular liposomes appear to be an excellent mimic of the Z rings in bacterial cells, but so far they are only found in multi-lamellar tubular liposomes, which are not frequent. The concave depressions and tubulation reaction are much easier to achieve, and the majority of liposomes on the slide show the same response. This system has already provided new evidence that protofilament bending is the basis of the constriction force. It will be a new tool to explore the mechanisms of Z-ring assembly and force generation.

## Materials and methods

### Expression and purification of membrane-targeted FtsZ

FtsZ-YFP-*mts* is a chimeric protein composed of FtsZ truncated after aa 366 (eliminating the FtsA-binding peptide), followed by YFP (Venus; Nagai *et al*, 2002) and a *mts*, the amphipathic helix from *E. coli* MinD. The *mts* we used included aa's 255–270 (IEEEKKGFLLKRLFGG, although the actual amphipathic helix includes aa's 261–268; Szeto *et al*, 2003). FtsZ-YFP-*mts* and FtsZ-*mts* (without YFP) were initially constructed in plasmid pJSB2 (Redick *et al*, 2005) by conventional recombination techniques. To obtain protein for *in vitro* studies, we used PCR to transfer these constructs to the pET11b expression vector (Invitrogen), at the *NdeI/BamHI* sites. The final amino-acid sequences are FtsZ (1–366)—pprpaggr—YFP—ggr—*mts* for FtsZ-YFP-*mts* and FtsZ (1–366)—pprpaggr—*mts* for FtsZ-*mts*, where the lowercase indicates aa's added in cloning. We also fused the *mts* to the N-terminus of FtsZ-YFP (*mts*-FtsZ-YFP). To create the *mts*-FtsZ-YFP, first FtsZ-YFP was cloned into pET15b at the *NdeI/BamHI* sites, which fused a His tag to the N-terminus. Then *mts* was substituted for the His tag region using the *NcoI/NdeI* sites. We made two kinds of *mts*-FtsZ-YFP. One has a single aa (His) and another has a 43-aa insertion between the *mts* and FtsZ. The final sequence is mggr—*mts*—hmtsgatglgefghmtsgatglgefghmtsgatglgefgh (or just h for the 1-aa insertion)—FtsZ—gst—YFP for the 43-aa insertion. The expression vectors were transformed into in *E. coli* strain C41 (Miroux and Walker, 1996) and protein expression was induced

at 20°C by addition of 0.5 mM IPTG. FtsZ-mts was a relatively well-behaved expression protein that was recovered mostly in the soluble fraction from the lysed bacteria. It was purified by precipitation with 30% saturated ammonium sulphate and chromatography on a Source Q (GE Healthcare) column. The purified protein was dialysed into HMK350 buffer (50 mM HEPES/KOH, pH 7.7, 5 mM MgAc, 350 mM KAc) and stored at -80°C. Some experiments used HMK100, in which KAc was 100 mM.

For the experiments reported here, FtsZ-YFP-mts was prepared by denaturation in guanidine-HCl and renaturation, as described previously (Osawa *et al*, 2008). We used the more complex renaturation protocol because an early preparation of soluble native protein had no activity. However, we have recently found that the native FtsZ-YFP-mts, purified as described above for FtsZ-mts, had full activity and was indistinguishable from renatured FtsZ-YFP-mts in both Z-ring formation inside tubular liposomes and in the liposome tubulation assay. We now prefer the native preparation for its simplicity and high yield.

Renatured FtsZ-YFP-mts is sensitive to buffer conditions. For tubulation experiments, protein in column buffer was diluted 10 × or more into HMK100/350. Dialysing renatured FtsZ-YFP-mts into HMK350 led to aggregation of the protein and loss of activity. We later found that this could be avoided if we kept 10% glycerol and 50 mM chloride in the dialysis buffer. We now use HMKCG buffer (50 mM HEPES/KOH, pH 7.7, 5 mM MgAc, 300 mM KAc, 50 mM KCl, 10% glycerol) for dialysis or long-term experiments. This precaution was needed for the renatured FtsZ-YFP-mts, but seems not necessary for native FtsZ-YFP-mts, FtsZ-mts or FtsZ. Once diluted into HMK350, however, the tubulation activity of renatured FtsZ-YFP-mts was stable for at least 24 h. For short term experiments, we used HMK100/350.

#### Liposome preparation

DOPG, egg PC and *E. coli* Polar Lipid Extract were purchased from Avanti. For some experiments, large multi-lamellar vesicles were prepared from a mixture of DOPG and PC at a 20:80 ratio (w/w). The lipids were dissolved in methanol, dried in a 1.5-ml Eppendorf tube and resuspended in water at 10 mg/ml by vigorous vortexing. A 250-μl volume of this suspension was placed in the form of many small (5 μl) drops on a 3.7-cm diameter Teflon disc. The drops were completely dried by air current and then hydrated by putting the disc in a small beaker and covering with 5 ml HMK100/350 buffer or HMKCG. Large liposomes (~5 μm diameter) were formed during incubation at 37°C for 6 h. We collected the white, cloudy solution near the disk, which had the most concentrated liposomes.

## References

- Allard JF, Cytrynbaum EN (2009) Force generation by a dynamic Z-ring in *Escherichia coli* cell division. *Proc Natl Acad Sci USA* **106**: 145–150
- Anderson DE, Gueiros-Filho FJ, Erickson HP (2004) Assembly dynamics of FtsZ rings in *Bacillus subtilis* and *Escherichia coli* and effects of FtsZ-regulating proteins. *J Bacteriol* **186**: 5775–5781
- Bi E, Lutkenhaus J (1991) FtsZ ring structure associated with division in *Escherichia coli*. *Nature* **354**: 161–164
- Bustamante C, Marko JF, Siggia ED, Smith S (1994) Entropic elasticity of lambda-phage DNA. *Science* **265**: 1599–1600
- Chen Y, Erickson HP (2005) Rapid *in vitro* assembly dynamics and subunit turnover of FtsZ demonstrated by fluorescence resonance energy transfer. *J Biol Chem* **280**: 22549–22554
- Chen Y, Erickson HP (2009) FtsZ filament dynamics at steady state subunit exchange with and without nucleotide hydrolysis. *Biochemistry* **48**: 6664–6673
- Cordell SC, Robinson EJ, Lowe J (2003) Crystal structure of the SOS cell division inhibitor Sula and in complex with FtsZ. *Proc Natl Acad Sci USA* **100**: 7889–7894
- Dajkovic A, Lan G, Sun SX, Wirtz D, Lutkenhaus J (2008) MinC spatially controls bacterial cytokinesis by antagonizing the scaffolding function of FtsZ. *Curr Biol* **18**: 235–244
- de Boer P, Crossley R, Rothfield L (1992) The essential bacterial cell division protein FtsZ is a GTPase. *Nature* **359**: 254–256
- Erickson HP (1997) FtsZ, a tubulin homolog, in prokaryote cell division. *Trends Cell Biol* **7**: 362–367
- Erickson HP (2009) Modeling the physics of FtsZ assembly and force generation. *Proc Natl Acad Sci USA* **106**: 9238–9243
- Erickson HP, Taylor DW, Taylor KA, Bramhill D (1996) Bacterial cell division protein FtsZ assembles into protofilament sheets and minirings, structural homologs of tubulin polymers. *Proc Natl Acad Sci USA* **93**: 519–523
- Farsad K, De Camilli P (2003) Mechanisms of membrane deformation. *Curr Opin Cell Biol* **15**: 372–381
- Higgins MK, McMahon HT (2005) *In vitro* reconstitution of discrete stages of dynamin-dependent endocytosis. *Methods Enzymol* **404**: 597–611
- Horger I, Velasco E, Mingorance J, Rivas G, Tarazona P, Velez M (2008) Langevin computer simulations of bacterial protein filaments and the force-generating mechanism during cell division. *Phys Rev E Stat Nonlin Soft Matter Phys* **77**: 011902
- Hu Z, Gogol EP, Lutkenhaus J (2002) Dynamic assembly of MinD on phospholipid vesicles regulated by ATP and MinE. *Proc Natl Acad Sci USA* **99**: 6761–6766
- Lan G, Daniels BR, Dobrowsky TM, Wirtz D, Sun SX (2009) Condensation of FtsZ filaments can drive bacterial cell division. *Proc Natl Acad Sci USA* **106**: 121–126
- Lan G, Wolgemuth CW, Sun SX (2007) Z-ring force and cell shape during division in rod-like bacteria. *Proc Natl Acad Sci USA* **104**: 16110–16115
- Miroux B, Walker JE (1996) Over-production of proteins in *Escherichia coli*: mutant hosts that allow synthesis of some membrane proteins and globular proteins at high levels. *J Mol Biol* **260**: 289–298

The liposomes prepared with HMK100 were usually diluted 1/10. Multi-lamellar liposomes prepared with HMK350 were at a lower concentration and were not diluted. For a typical tubulation experiment, 4 μM FtsZ-YFP-mts and 400 μM GTP were added to the liposome suspension in HMK100/350 or HMKCG.

Alternatively, small unilamellar liposomes were prepared using a membrane extruder (Avanti; Higgins and McMahon, 2005) equipped with a polycarbonate filter (Whatman, pore size 0.8 μm). A 10 mg/ml suspension of lipid in HMK350 was processed with the extruder and was later diluted before use. This method was used for all experiments where the lipid was quantitated.

#### Light microscopy

A Zeiss Axiophot with ×100 magnification and 1.3 NA objective was used for differential interference contrast and fluorescence microscopy. A filter cube optimized for YFP was used for fluorescence microscopy. Images were acquired with a Coolsnap HQ charge-coupled device camera (Roper Scientific). Liposomes were observed after applying a coverslip to a small drop of the suspension.

#### FRAP assay

FRAP assays were performed with a Zeiss LSM Live DuoScan confocal microscope with a dedicated bleaching laser. The data were converted to stacked TIFF files using ImageJ (NIH) and fluorescence intensities in the specific areas were analysed with Metamorph (Molecular Devices). Each recovery curve was fitted to a single-exponential equation and recovery half-times were determined as previously described (Anderson *et al*, 2004).

#### Electron microscopy

Tubulating liposomes with FtsZ-YFP-mts were observed by conventional negative staining methods. A 10-μl volume of reaction mixture was applied to a carbon-coated grid and stained with two drops of 2% aqueous uranyl acetate. Images were recorded photographically at a magnification of ×50 000.

#### Supplementary data

Supplementary data are available at *The EMBO Journal* Online (<http://www.embojournal.org>).

## Acknowledgements

This work was supported by NIH Grant GM66014.

- Moores CA, Milligan RA (2008) Visualisation of a kinesin-13 motor on microtubule end mimics. *J Mol Biol* **377**: 647–654
- Mukherjee A, Dai K, Lutkenhaus J (1993) *Escherichia coli* cell division protein FtsZ is a guanine nucleotide binding protein. *Proc Natl Acad Sci USA* **90**: 1053–1057
- Mukherjee A, Lutkenhaus J (1994) Guanine nucleotide-dependent assembly of FtsZ into filaments. *J Bacteriol* **176**: 2754–2758
- Nagai T, Ibata K, Park ES, Kubota M, Mikoshiba K, Miyawaki A (2002) A variant of yellow fluorescent protein with fast and efficient maturation for cell-biological applications. *Nat Biotechnol* **20**: 87–90
- Ohashi T, Galiacy SD, Briscoe G, Erickson HP (2007) An experimental study of GFP-based FRET, with application to intrinsically unstructured proteins. *Protein Sci* **16**: 1429–1438
- Osawa M, Anderson DE, Erickson HP (2008) Reconstitution of contractile FtsZ rings in liposomes. *Science* **320**: 792–794
- Osawa M, Erickson HP (2009) Tubular liposomes with variable permeability for reconstitution of FtsZ rings. *Methods Enzymol* **464** (in press)
- Pichoff S, Lutkenhaus J (2005) Tethering the Z ring to the membrane through a conserved membrane targeting sequence in FtsA. *Mol Microbiol* **55**: 1722–1734
- RayChaudhuri D, Park JT (1992) *Escherichia coli* cell-division gene *ftsZ* encodes a novel GTP-binding protein. *Nature* **359**: 251–254
- Redick SD, Stricker J, Briscoe G, Erickson HP (2005) Mutants of FtsZ targeting the protofilament interface: effects on cell division and GTPase activity. *J Bacteriol* **187**: 2727–2736
- Romberg L, Simon M, Erickson HP (2001) Polymerization of FtsZ, a bacterial homolog of tubulin. Is assembly cooperative? *J Biol Chem* **276**: 11743–11753
- Saarikangas J, Zhao H, Pykalainen A, Laurinmaki P, Mattila PK, Kinnunen PK, Butcher SJ, Lappalainen P (2009) Molecular mechanisms of membrane deformation by I-BAR domain proteins. *Curr Biol* **19**: 95–107
- Shimada A, Niwa H, Tsujita K, Suetsugu S, Nitta K, Hanawa-Suetsugu K, Akasaka R, Nishino Y, Toyama M, Chen L, Liu ZJ, Wang BC, Yamamoto M, Terada T, Miyazawa A, Tanaka A, Sugano S, Shirouzu M, Nagayama K, Takenawa T, Yokoyama S (2007) Curved EFC/F-BAR-domain dimers are joined end to end into a filament for membrane invagination in endocytosis. *Cell* **129**: 761–772
- Sweitzer SM, Hinshaw JE (1998) Dynamin undergoes a GTP-dependent conformational change causing vesiculation. *Cell* **93**: 1021–1029
- Szeto TH, Rowland SL, Habrukowich CL, King GF (2003) The MinD membrane targeting sequence is a transplantable lipid-binding helix. *J Biol Chem* **278**: 40050–40056
- Takei K, Haucke V, Slepnev V, Farsad K, Salazar M, Chen H, De Camilli P (1998) Generation of coated intermediates of clathrin mediated endocytosis on protein-free liposomes. *Cell* **94**: 131–141
- Tan D, Rice WJ, Sosa H (2008) Structure of the kinesin13-microtubule ring complex. *Structure* **16**: 1732–1739
- Wang HW, Nogales E (2005) Nucleotide-dependent bending flexibility of tubulin regulates microtubule assembly. *Nature* **435**: 911–915